Calculation of Inrush Currents – Benchmarking of Transformer Models

N. Chiesa, H. K. Høidalen, M. Lambert, M. Martínez Duró

***Abstract*–The paper investigates the behavior of four transformer models in electromagnetic transients programs (EMTP) when calculating inrush currents due to shell-type transformers energization. These models are single-phase Saturable Transformer (STC), BCTRAN, Hybrid Transformer (XFMR) and UMEC. The measurements of a real transformer energization performed by EDF in France are used to evaluate the accuracy of the simulation results provided by each model. For the first periods of the inrush, the results show that only a topologically correct transformer model as the hybrid transformer model is able to reproduce the current amplitude in the three phases and the overall wave shape. BCTRAN, STC and UMEC may predict the first inrush current peak, but the amplitudes in the other two phases are far from the measurements. The current decay in the 2 seconds after the energization is poorly predicted by all of the models underlining a poor losses representation in the transformer model and in the rest of the network.**

***Keywords*: Power transformers, inrush currents, measurements, simulations, ATP, EMTP-RV, PSCAD/EMTDC.**

I. INTRODUCTION

TRANSIENT energization studies of transformers are important for power system reliability consideration and particularly for the design of power system restoration strategies after blackout. During power system restoration, the supplying network exhibits high harmonic impedance; therefore, the inrush currents may generate dangerous temporary overvoltages that could damage the transformers or other equipment [1].

However, the standard available models in EMT-type programs could in many cases have insufficient accuracy and capabilities. Uncertainties are in estimating the residual fluxes, the behavior in extreme saturation, the dependence of core structure, and the influence of multi-windings designs [2].

In this paper, the simulation results obtained for various standard available transformer models in ATP, EMTP-RV and PSCAD/EMTDC are compared to the measured inrush current of a real energization performed at EDF in France.

This work received partial financial support from the KMB project "Electric power systems for subsea processing and transportation of oil and gas" financed by the Norwegian Research Council Petromaks programme and industry partners (www.subseapowersupply.com).

N. Chiesa is with SINTEF Energy Research, Trondheim, Norway (e-mail of corresponding author: nicola.chiesa@sintef.no).

H. K. Høidalen is with the Norwegian University of Science and Technology, N-7491 Trondheim, Norway (hans.hoidalen@elkraft.ntnu.no).

M. Lambert is with Ecole Polytechnique de Montréal, Canada (mathieu.lambert@polymtl.ca).

M. Martínez Duró is with Electricité de France, R&D Division, Clamart, France (manuel.martinez@edf.fr).

Paper submitted to the International Conference on Power Systems Transients (IPST2011) in Delft, the Netherlands June 14-17, 2011

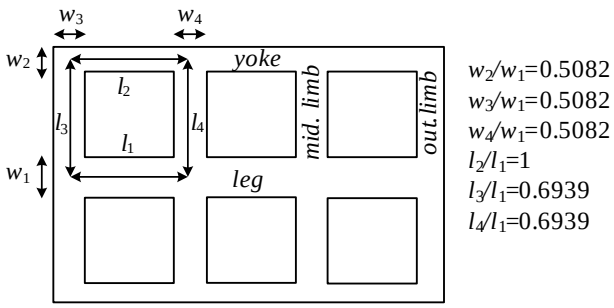

Fig. 1. Shell-form core and relative core dimensions.

II. TRANSFORMER MODELS

The test object is a 96 MVA four-winding auxiliary transformer with a shell-type core. The transformer is energized from its primary 400 kV Y-coupled winding. The secondary side consists of three 6.8 kV delta-coupled windings.

Available data for the modeling of the transformer are the standard test report shown in Table I, relative core dimensions and the air-core inductance. The relative core dimensions are shown in Fig. 1. The air-core inductance provided by the manufacturer is 1.4 H referred to the HV side. The tap-changer position is set to tap 1, corresponding to 410 kV. Since there is no tap-changer option in the selected models, the tap-changer voltage is specified as nominal voltage.

The three secondary windings are merged into one equivalent winding in order to be able to implement the transformer in models that are limited to two- or three-windings. This is plausible since the three windings are identical and are considered as connected in parallel.

The target transformer is represented with the Saturable Transformer Component (STC), BCTRAN, Hybrid Trans-

TABLE I
AUXILIARY TRANSFORMER'S TEST REPORT

Main data	[kV]	[MVA]	[A]	Coupling
HV	400±2.5%	96	138.6	YN
LV	6.8	96	8151	d11
Open-circuit	E_0 [%]	[MVA]	I_0 [%]	P_0 [kW]
LV	90	96	0.171	75.25
	100	96	0.421	101.5
	105	96	0.634	117.0
	110	96	0.971	137.8
	115	96	1.601	165.6
Short-circuit	[kV]	[MVA]	E_k [%]	P_k [kW]
HV/LV	410/6.8*	96	5.59	332.95

* The test with all three LV windings paralleled and shorted is used.

former (XFMR), and UMEC models. Among these, only the XFMR model can handle a shell-type core topology directly. For comparison, a triplex core equivalent is considered for both XFMR and UMEC cases. Single-phase transformer models cannot account for differences in direct- and zero-sequence behavior of three-phase single-core transformers. However, a triplex representation may be enough if a delta winding is present and rules the zero-sequence behavior of the transformer [3]. Furthermore, for shell-type and four- or five-limb cores, the core provides an unwounded return path for the phase flux. Therefore, differences between direct- and zero-sequence behaviors are less significant than for three-legged cores.

A. Saturable transformer model

The Saturable Transformer Component (STC) [2], [4] is a two- and three-winding single phase transformer model. It is the nonlinear version of the classic Steinmetz model [5]. It represents the short-circuit impedances between windings, the load and magnetization losses, and the nonlinear inductive magnetization. When it is used to model three-phase transformers, the inter-phase magnetic coupling is not represented in this model. STC is based on an equivalent star circuit where the core representation can be connected either to the star point or to the terminal of the winding closest to the core. This model may suffer from instability problem when three windings are modeled and the core is connected to the star point [4], [6]. As proven in [7], this model is not valid for more than three windings per phase. The STC model is implemented in both ATP and EMTP-RV. This model is available in PSCAD as transformer model based on "classical modeling approach (not ideal)".

In this paper, the core representation is connected at the star point, in-between the separated leakage reactances and winding resistances (the short-circuit impedance). While in ATP and EMTP-RV the nonlinear inductances are modeled with piecewise-linear characteristic, in the PSCAD model the they are modeled as a two-slope characteristic. The winding resistance and leakage inductance are equally split on a p.u. base between primary and secondary winding (0.5 splitting factor) [4].

B. BCTRAN model

The BCTRAN model [8] is a n-phase transformer model where inter-winding coupling can be taken into account. The model is linear and assumes phase symmetry. It consists of a coupled RL or RL^{-1} matrix representing short-circuit impedances between windings, load losses at rated frequency and optionally linear inductive magnetization. Nonlinear magnetization and core loss components may be added externally, usually at the terminals of the winding nearest to the core.

BCTRAN is implemented in EMTP-RV, ATP. In PSCAD is available as transformer model based on "classical modeling approach (ideal)". In PSCAD, the classical transformer model allows only for a two-slope saturation curve. The EMTP-RV and ATP implementation of BCTRAN is investigated here as it offers better control over the magnetization characteristic through external nonlinear inductances.

In this paper, the core representation is connected to the LV winding terminal in a delta configuration.

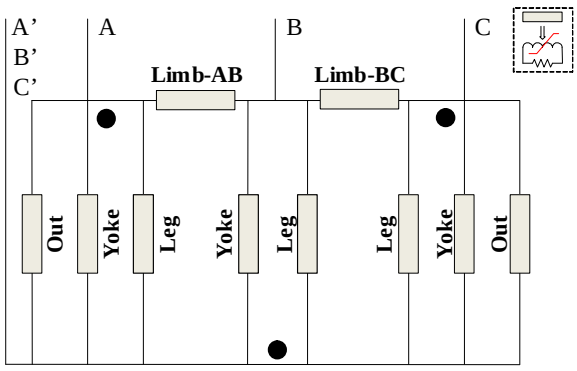

Fig. 2. Shell-form core model in the Hybrid Transformer.

C. Hybrid transformer model

The Hybrid Transformer model [9]–[11] is an engineering transformer model based on limited input data, available in ATPDraw. The duality-derived electrical circuit of a shell-form core is shown in Fig. 2. In Test Report mode, the model requires data like the one given in Table I and the magnetization curve is fitted to a modified Frolich equation [11] internally.

The relative core dimensions must be entered according to Fig. 1, except that the relative areas must be multiplied by a factor of 2. Since relative widths in Fig. 1 are equal for the outer legs, yokes and middle limbs, the middle phase's polarity has to be reversed to get 1 p.u. flux in all core parts, as shown in Fig. 2 (shell-form type B in ATPDraw version $>$5.7).

In the present case, the air-core inductance is specified and the final slope of the magnetization characteristic is approximated by [12]:

$$L_{\infty} \approx L_{air-core} - (1+k)L_{HL} \tag{1}$$

where L_{HL} is the short circuit inductance from the test report and k is a calibration factor representing the leakage between the inner winding and the core assumed to be 0.5 in the Hybrid Model. This gives $L_{\infty} = 0.8295$ mH referred to the LV side.

D. UMEC model

The UMEC transformer model [13], [14] is based on the concept of a unified magnetic equivalent circuit. A normalized core is used in order to remove the requirement of design data; only relative dimensions are required.

The magnetic network is derived from the transformer core topology. Three-limb, five-limb, and three-phase bank (triplex) transformer core constructions are possible configurations in the model. The core saturation characteristic is specified directly as a rms I-V curve. The magnetic network representing the core and leakage inductances is described with a matrix formulation using a permeance matrix. Both the

magnetic coupling between windings of different phases and the coupling between windings of the same phase are taken into account.

Winding and core losses are not included in the magnetic circuit and are represented by an equivalent linear resistance at the winding terminals. Load losses are equally divided on a p.u. base and represented by linear series resistances connected at one terminal of each winding. Core losses are assumed linear and equally divided on a p.u. base between primary and secondary windings. The use of a magnetic network does not allow a simple representation of topological core losses, therefore they are represented by linear shunt resistances connected at the terminals of each winding.

The UMEC model is implemented in PSCAD.

E. Saturation curves and open-circuit model responses

One of the most critical steps in the creation of a transformer model for inrush current calculation is the construction of the saturation curves accounting for the nonlinear behavior of the core. These are calculated to match the open-circuit test data of Table I.

A routine for the conversion from rms to peak value [15] is used for the generation of the saturation curve required by BCTRAN and STC. An additional point is defined beyond the last calculated value to set the saturated inductance according to the air-core inductance:

$$L_{sat} = L_{air-core} - L_{HL} \tag{2}$$

and resulting in the curve shown in Fig. 3. For the STC model, the saturated inductance is calculated by removing only a fraction of the total leakage inductance L_{HL}, corresponding to the fraction of leakage placed on the primary side:

$$L_{sat} = L_{air-core} - \xi\, L_{HL} \tag{3}$$

where ξ is the fraction of total leakage placed on the primary side.

In XFMR, the conversion from open-circuit test data to saturation curve is performed by a sophisticated algorithm based on a curve fitting approach. The resulting saturation curves are shown in Fig. 3 for the triplex and shell topologies. For the shell-core transformer case, four saturation curves are calculated by the XFMR model based on the relative area and length of each limb. One may see in Fig. 3 that for the same flux-linkage value the curve fitting approach used in XFRM leads to lower magnetization currents than those obtained with curves where L_{sat} is located right after the last magnetization point.

Similarly to XFMR, the UMEC model has also the ability to create the saturation curves from open-circuit data. In Fig. 4 the curves labeled "UMEC (orig)" are with direct input of test report data according to Table I. As also pointed out in [10] the input has to be conditioned to match the no-load test data. In Fig. 4 the curves labeled "UMEC (cond)" are obtained by specifying the saturation curve labeled "BCTRAN & STC" in Fig. 3, scaled by $\sqrt{3/2}$ for the current and $\omega/\sqrt{2}$ for the flux-linkages.

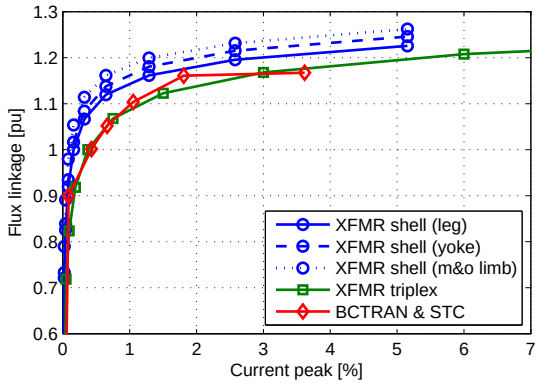

Fig. 3. Saturation curves.

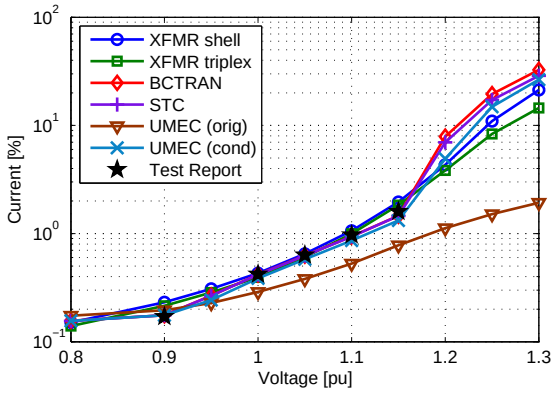

(a) No-load current.

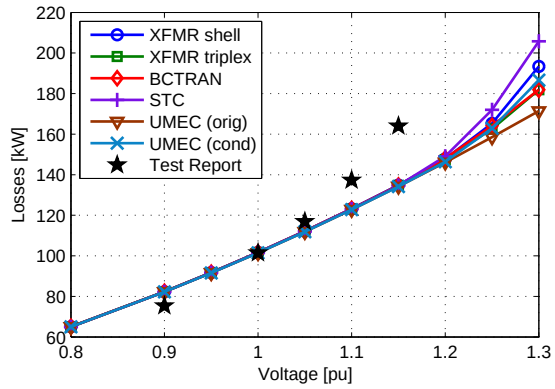

(b) No-load losses.

Fig. 4. Open circuit test of the transformer models compared to input test report values.

For all models, the core losses are modeled with linear resistor to match the losses at rated excitation. Nonlinear resistors could be used to match more accurately the nonlinear loss behavior; however, their transient performances is somewhat uncertain [16].

Open-circuit tests of the transformer models are performed to ensure the accurate match with the input data of Table I. With the exception of the original UMEC model, all models can accurately match the input no-load current values as shown in Fig. 4(a). The area beyond the last known point shows that

some uncertainties and discrepancies can be observed with the different models. Fig. 4(b) shows the simulated no-load losses versus the test report input values. All models can match the losses at rated excitation and again some differences can be noticed at higher excitation.

III. TEST CASE

A. Network topology

The field test network used to benchmark the transformer models is represented in Fig. 5. The unloaded auxiliary transformer at the target plant is energized from a supplying network consisting in a 315 km 400 kV overhead line fed by a source plant. The source plant's step-up transformer consists of three single-phase units rated 550 MVA each. The source plant's auxiliary transformer is identical to the one at the target plant and is loaded. The overhead line is double-circuit (albeit only one is energized) and untransposed. Two iron-core compensation reactors of 100 MVAr each are present near the target plant.

The network supplying the energized transformer is modeled according to the findings in [17]. The generator is modeled by an ideal voltage source behind an impedance accounting for the subtransient reactance and the armature resistance. The step-up transformer is modeled with single-phase transformer models with nonlinear core. The overhead line is modeled by cascaded PI cells calculated at the power frequency (50 Hz) from the conductors' geometrical and physical characteristics. The compensation reactances are modeled as constant inductances (they are linear in the voltage range of the measurements) with parallel resistances accounting for losses.

B. Measurements

The measurements include LV-side voltages at the de-energization of the transformer and HV-side voltages and currents at the energization, as well as induced LV-side voltages. The flux-linkages are calculated as the time integral of the LV-side voltages. The measured waveforms and the calculated flux-linkages are shown in Figs. 6-7. Throughout the paper, the colors blue, green, and red are used to identify the waveforms for phase A, B and C, respectively.

Inrush currents and subsequent harmonic overvoltages are highly dependent on two initial conditions: residual fluxes of

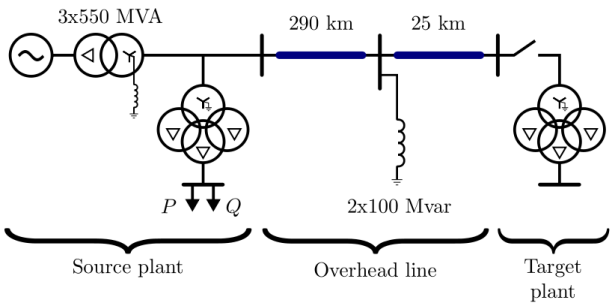

Fig. 5. Field test case.

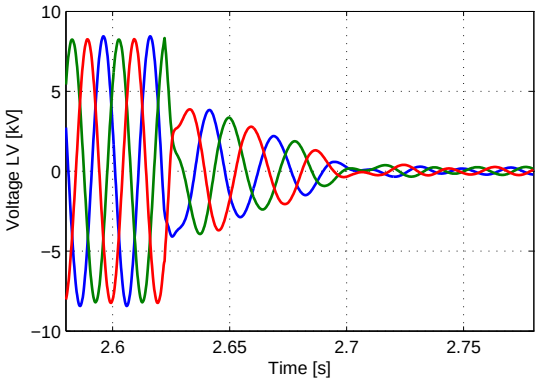

(a) Voltages at the LV-side of the transformer.

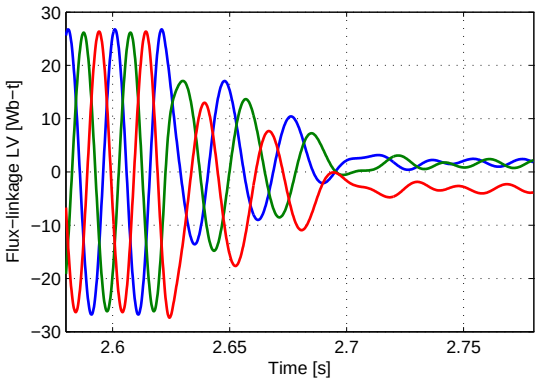

(b) Flux-linkages (referred to the LV-side) and final residual fluxes.

Fig. 6. Measurements of de-energization transient.

the energized transformer and switching times of the circuit-breaker. The switching times were obtained by identifying sudden changes of the voltages at the terminals of the transformer. A delay in the poles of the breaker is observed from the measurements where phase B and C close 11.6 ms after phase A.

Fig. 6 highlights a rather long ring-down transient lasting a few periods, supposedly due to large transformer capacitances [18], resulting in relatively low final residual fluxes. The residual fluxes estimated from the flux-linkages after the ringdown transient are 6.3%, 5.5%, and -10.2% of the rated flux, respectively for the three phases. Due to their low values, they have been neglected in the simulations.

IV. RESULTS

A. Inrush current waveforms

Figs. 8-13 show the first four periods of the inrush current waveforms calculated with the different models. Each curve is compared with the measured inrush current.

In general, all the models based on a triplex or single phase representation give similar results in terms of current amplitude and shape of the waveforms as shown in Fig. 8, Fig. 9, Fig. 11 and Fig. 13. STC, BCTRAN, and UMEC (with conditioned data) give very similar result as they are based on the same saturation curve (Fig. 3). In XFMR with triplex core, the current is slightly lower due to a higher saturation

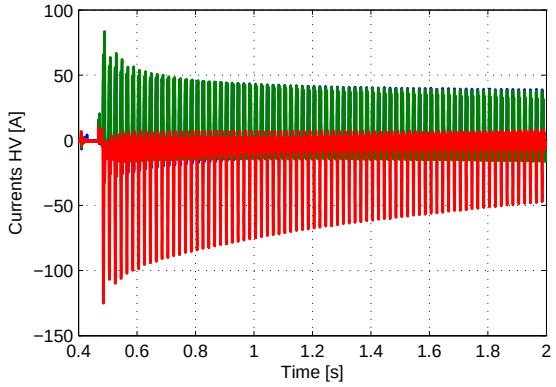

(a) Inrush current for the target transformer.

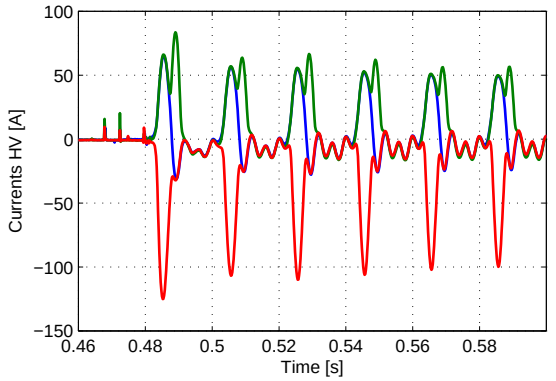

(b) Close-up of measured inrush current.

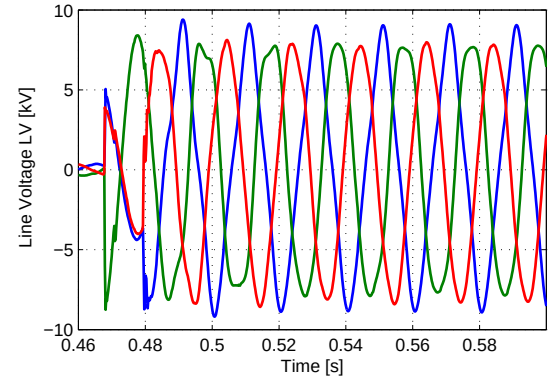

(c) Induced voltages on the transformer LV-side.

Fig. 7. Measurements of the energization transient.

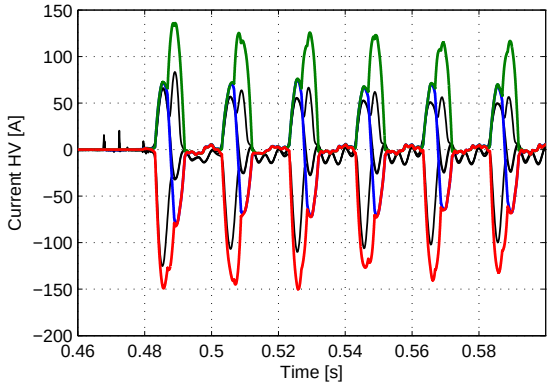

Fig. 8. Inrush current with STC. Color lines: simulation. Black lines: Measurements.

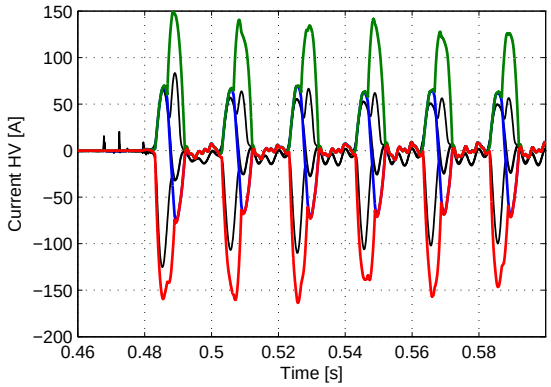

Fig. 9. Inrush current with BCTRAN. Color lines: simulation. Black lines: Measurements.

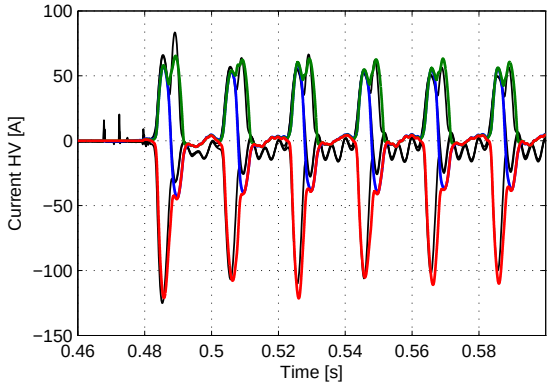

Fig. 10. Inrush current with XFMR (shell core). Color lines: simulation. Black lines: Measurements.

curve. The inrush currents calculated with these models are relatively close to the first peak of phase C. However, they fail to reproduce the other phases' first peak and the overall shape of the waveforms. The simulation results obtained with the XFMR model using a topologically correct shell-core model can match both the inrush current and waveform shape in the first periods of the inrush transient, as shown in Fig. 10.

Fig. 12 shows that the UMEC model does not succeed to accurately represent inrush transient when no-load data are not conditioned.

Fig. 14 shows the induced voltage on the LV-side and compares the simulation result obtained with XFMR (shell) with the measurements. Since there is no significant overvoltage, voltages are less sensitive than currents and similar waveforms are obtained with all the analyzed models.

B. Current Decay

The absolute value of the inrush current envelope for the first two seconds after the energization of the transformer is shown in Fig. 15 for the considered models, as well as for the measurements. All the models can poorly predict the current decay. Curves are all parallel reflecting that the models have similar losses' representation (linear winding and core losses). The only exception is BCTRAN as it has a much larger decay

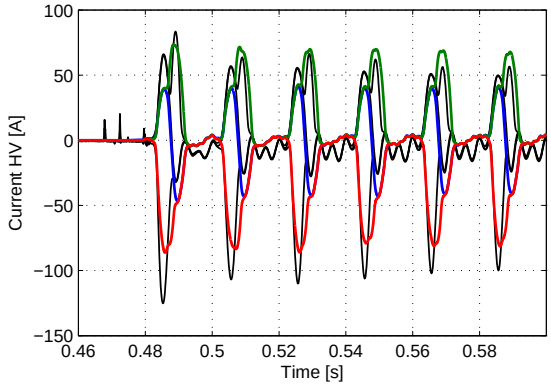

Fig. 11. Inrush current with XFMR (triplex). Color lines: simulation. Black lines: Measurements.

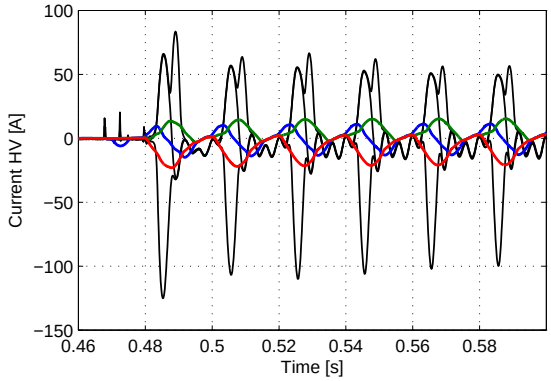

Fig. 12. Inrush current with UMEC (original data). Color lines: simulation. Black lines: Measurements.

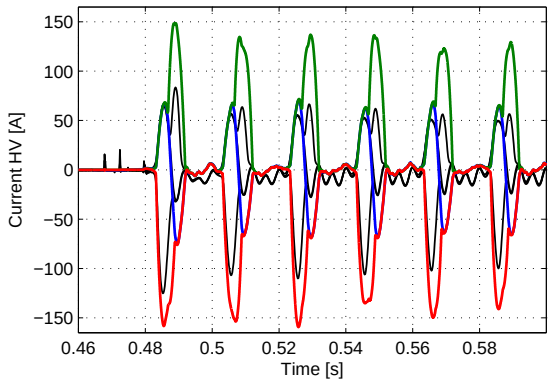

Fig. 13. Inrush current with UMEC (conditioned data). Color lines: simulation. Black lines: Measurements.

than the other models. In BCTRAN, the core is connected to the LV winding. Therefore, current flows in both HV and LV winding resistances. This gives higher losses and faster current decay. Hence, it is incorrect as only the current's zero-sequence component of the current should circulate in the LV winding; therefore, the contribution to the inrush current damping is minimal.

C. Inrush patterns

The simulations presented until now are representative of a single switching sequence. In order to better investigate the

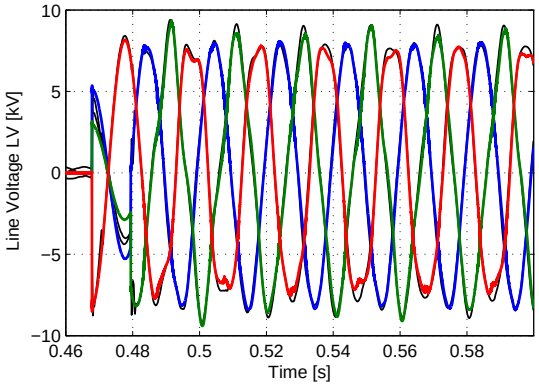

Fig. 14. Induced LV-side voltages with XFMR (shell core). Color lines: simulation. Black lines: Measurements.

effect of the switching instant, the inrush current patterns for the case of zero residual flux are presented in Fig. 16 and Fig. 17. These patterns are obtained by varying the switching in instant with the introduction of a delay between 0 and 20 ms. Then the maximum inrush current is recorded and plotted as a function of the switching in delay. The time t=0 is equivalent to the test case switching instant.

Fig. 16 shows the inrush current pattern when a delay of 11.6 ms is maintained between the first pole to close (phase A) and the other two poles. From this figure, it is evident that the analyzed test case (in t=0) is close to the maximum inrush current for phase C, but is less than half the most severe inrush current that can be experienced by this transformer.

The effect of a different delay between the circuit breaker poles is also shown in Fig. 16. The thinner lines show the inrush pattern for poles delay of 10.6 and 12.6 ms. The inrush current first peak is highly sensitive to a variation of this parameter.

Fig. 17 compares the inrush pattern obtained with XFMR (shell core) and BCTRAN for simultaneous three-pole closing. The two models predict a similar maximum inrush current for the transformer of about 220 A (1.15 p.u.). While BCTRAN predicts an equal pattern for the three phases, XFMR with its topologically-correct shell-core representation can calculate a lower current for the middle phase. While the maximum inrush current estimated by the two models is fairly similar, at specific switching instants the difference can be up to 200%.

V. Discussion

The transformer models analyzed in this paper can estimate the first peak of the inrush current with good accuracy. The main reasons are the knowledge of the air-core inductance (provided by the manufacturer) and the availability of an extensive no-load test report (with maximum induction level of 115%).

The knowledge of the air-core inductance allows to treat the final slope of the saturation curve equally in all models. At 115% excitation, the current is only few per-cent of the rated current. However, during inrush current transients the current peaks are in excess of the rated current. The unknown area beyond the last known point in the saturation curve

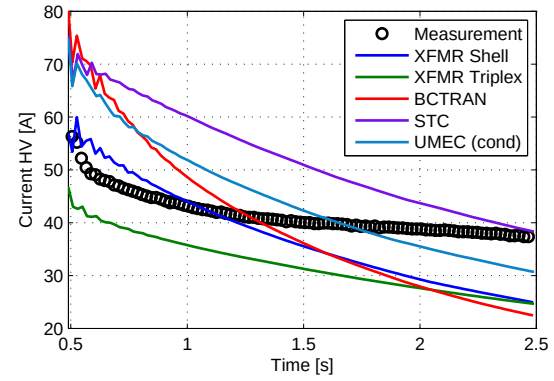

(a) Phase A

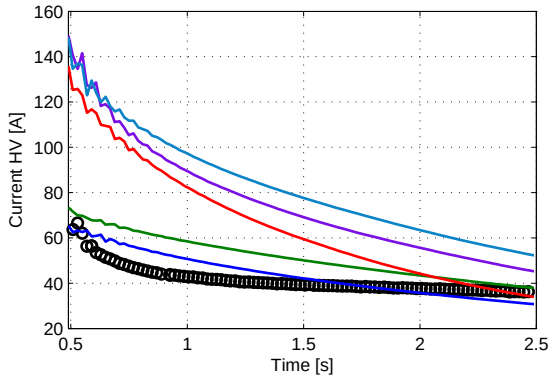

(b) Phase B

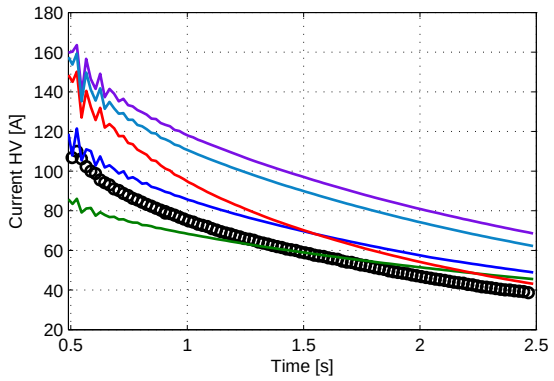

(c) Phase C

Fig. 15. Inrush current decay, 2 s.

is therefore critical for the accuracy of the inrush current estimation. As outlined in [12], [19], an accurate representation of the saturation and its final slope is of uttermost importance for the simulation of transformer energization.

The main difference between the analyzed models is due to the approach used for the estimation of the saturation curve. In the STC, BCTRAN and UMEC models, the slope after the last test report value (115%) is constant and equal to L_{sat}, while in the XFMR model, the slope after this point decreases smoothly to reach asymptotically the value of L_{inf} (Frolich equation fitting).

In addition, the modeling approach of the core has shown to be important. The connection point of the core at the star-point

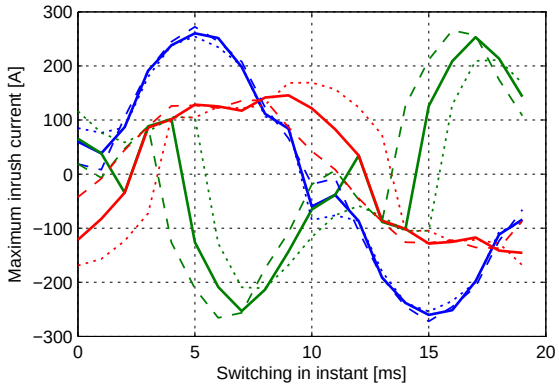

Fig. 16. Inrush current pattern with XFMR shell core. Continuous line: 11.6 ms delay. Dotted line: 10.6 ms delay. Dashed lines: 12.6 ms delay.

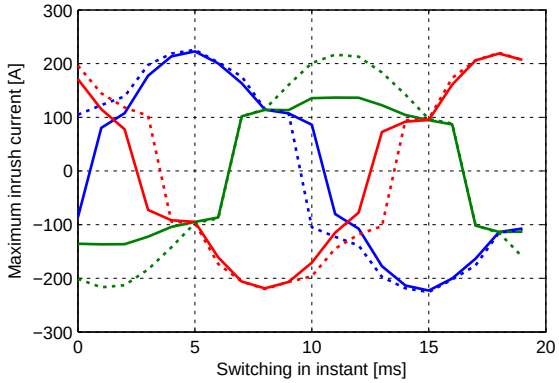

Fig. 17. Inrush current pattern. Continuous lines: XFMR shell core. Dotted lines: BCTRAN.

(STC), at the LV-terminals (BCTRAN) or at internal points (UMEC and XFMR) makes a difference in both the maximum inrush and the decay. The shell-form core's geometry is not too far away from that of a triplex core. However, the use of a topologically-correct shell-form core representation influences the waveform for the currents by considering asymmetries that exist between phases. This can be an important factor to take into consideration when overvoltages have to be analyzed, as they depend both on the current peak and the waveform.

The sensitivity of the simulation results to the switching instant is an important issue. Both switching instant and delay between each pole have to be accurately considered as they greatly influence the inrush current magnitude.

Residual flux is quite low as seen from the measurements and has not been taken into account in the analysis to avoid including an additional complicating factor. Initialization of nonlinear inductors, especially when included in topologically-correct core models, is still an issue and needs to be further investigated.

In order to improve the estimation of the inrush current decay, the loss modeling has to be greatly enhanced. This may be achieved with the use of frequency dependent winding resistances and the representation of nonlinear and topologically correct core losses. As shown in [19], the frequency dependent winding losses are important for transients between 0.1 Hz

and 3 kHz, while an accurate representation of hysteresis and iron losses may be unnecessary. Hence, a frequency-dependent winding-resistance model is required to represent the currents decay more accurately. The loss modeling in the other network components is also important.

VI. Conclusion

Several transformer models have been evaluated in their capability to accurately predict inrush currents due to the energization of three-phase shell-core transformers. These models are readily available in several simulation softwares. The evaluation consists in comparing the field measurements for a real transformer energization case performed at EDF and the simulation results provided by each model.

The simulation results show that a topologically correct core model is required if a higher accuracy is desired when simulating highly nonlinear and unbalanced electromagnetic transients. Good accuracy in the estimation of the inrush current's first peak can also be achieved with equivalent models if an accurate representation of the saturation and its final slope is employed.

In general, the investigated models manage to represent the inrush currents very well. The main reason is that no-load test report up to 115% excitation and air-core inductance were available. Hence, it is important for transformer owners to request such parameters when purchasing their units.

On the other hand, none of the examined models is able to match the current decay of the measurements. This issue would require further investigation. Particularly, the transformer core and load losses modeling would need to be improved in order to take into account nonlinear behavior and frequency dependency. The loss modeling of other network components is also important in the determination of the inrush current decay.

References

[1] D. Povh and W. Schultz, "Analysis of overvoltages caused by transformer magnetizing inrush current," *IEEE Trans. Power App. Syst.*, no. 4, pp. 1355–1365, Jul. 1978.

[2] J. A. Martinez and B. A. Mork, "Transformer modeling for low- and mid-frequency transients - a review," *IEEE Trans. Power Del.*, vol. 20, no. 2 II, pp. 1625–1632, 2005.

[3] M. R. Iravani, A. K. S. Chaudhary, W. J. Giesbrecht, I. E. Hassan, A. J. F. Keri, K. C. Lee, J. A. Martinez, A. S. Morched, B. A. Mork, M. Parniani, A. Sharshar, D. Shirmohammadi, R. A. Walling, and D. A. Woodford, "Modeling and analysis guidelines for slow transients. III. The study of ferroresonance," *IEEE Trans. Power Del.*, vol. 15, no. 1, pp. 255–265, 2000.

[4] H. W. Dommel and et.al., *Electromagnetic Transients Program Reference Manual (EMTP Theory Book)*. Portland, OR: Prepared for BPA, Aug. 1986.

[5] C. P. Steinmetz and E. J. Berg, *Theory and calculation of alternating current phenomena*. New York: Electrical World and Engineer, inc., 1897.

[6] T. Henriksen, "How to avoid unstable time domain responses caused by transformer models," *IEEE Trans. Power Del.*, vol. 17, no. 2, pp. 516–522, Apr. 2002.

[7] L. F. Blume, *Transformer engineering : a treatise on the theory, operation, and application of transformers*, 2nd ed. New York, N.Y.: John Wiley and Sons, Inc., 1951.

[8] V. Brandwajn, H. W. Dommel, and I. I. Dommel, "Matrix representation of three-phase n-winding transformers for steady-state and transient studies," *IEEE Trans. Power App. Syst.*, vol. PAS-101, no. 6, pp. 1369 –1378, June 1982.

[9] B. A. Mork, F. Gonzalez, D. Ishchenko, D. L. Stuehm, and J. Mitra, "Hybrid transformer model for transient simulation: Part I: development and parameters," *IEEE Trans. Power Del.*, vol. 22, no. 1, pp. 248–255, Jan. 2007.

[10] H. K. Høidalen, B. A. Mork, F. Gonzalez, D. Ishchenko, and N. Chiesa, "Implementation and verification of the hybrid transformer model in ATPDraw," *Electr. Power Syst. Res.*, vol. 79, no. 3, pp. 454 – 459, Mar. 2009, special Issue: Papers from the 7th International Conference on Power Systems Transients (IPST).

[11] H. K. Høidalen, N. Chiesa, A. Avendaño, and B. A. Mork, "Developments in the hybrid transformer model – Core modeling and optimization," in *IPST'2011*, 2011.

[12] N. Chiesa, B. A. Mork, and H. K. Høidalen, "Transformer model for inrush current calculations: Simulations, measurements and sensitivity analysis," *IEEE Trans. Power Del.*, vol. 25, no. 4, pp. 2599–2608, Oct. 2010.

[13] W. Enright, O. B. Nayak, G. D. Irwin, and J. Arrillaga, "An electromagnetic transients model of multi-limb transformers using normalized core concept," in *IPST'97 - International Conference on Power System Transients*, Seattle, Washington, Jun. 1997, pp. 93–98.

[14] W. Enright, O. Nayak, and N. Watson, "Three-phase five-limb unified magnetic equivalent circuit transformer models for PSCAD V3," in *IPST'99 - International Conference on Power System Transients*, Budapest, Hungary, Jul. 1999, pp. 462–467.

[15] N. Chiesa and H. K. Høidalen, "Analytical algorithm for the calculation of magnetization and loss curves of delta connected transformers," *IEEE Trans. Power Del.*, 2010, accepted for publication, TPWRD-00589-2009.

[16] N. Chiesa and H. K. Høidalen, "Hysteretic iron-core inductor for transformer inrush current modeling in EMTP," in *PSCC 2008 - 16th Power Systems Computation Conference*, Glasgow, Scotland, Jul. 2008.

[17] M. Martínez Duró, "Damping modeling in transformer energization studies for system restoration," in *PowerTech 2009*, Bucarest 2009.

[18] N. Chiesa, A. Avendaño, H. K. Høidalen, B. A. Mork, D. Ishchenko, and A. P. Kunze, "On the ringdown transient of transformers," in *IPST'07 - International Conference on Power System Transients*, no. IPST-229, Lyon, France, Jun. 2007.

[19] "Guidelines for representation of network elements when calculating transients," CIGRE WG 33.02, 1990.

Nicola Chiesa was born in Italy in 1980. He received the MSc degree in electrical Engineering from Politecnico di Milano in 2005, and the PhD degree from the Norwegian University of Science and Technology in 2010. He is now a research scientist at SINTEF Energy Research.

Hans Kr. Høidalen was born in Norway in 1967. He received his MSc and PhD from the Norwegian University of Science and Technology in 1990 and 1998 respectively. He is now a professor at the same institution with a special interest of electrical stress calculations and modeling.

Mathieu Lambert was born in Canada in 1984. He received his MSc from the Ecole Polytechnique de Montréal in 2009. He is now a PhD candidate at the same university.

Manuel Martínez Duró was born in Spain in 1975. He received the electrical engineering degree from the Universitat Politècnica de Catalunya, Barcelona, Spain, in 1999. He joined Electricité de France, R&D Division, France, in 2001.